Available online at www.sciencedirect.com
SCIENCE DIRECT®
Carbohydrate Research 339 (2004) 1973–1984
Carbohydrate RESEARCH

# Structural analysis of the lipopolysaccharide derived core oligosaccharides of *Actinobacillus pleuropneumoniae* serotypes 1, 2, 5a and the genome strain 5b

Frank St. Michael,[a] Jean-Robert Brisson,[a] Suzon Larocque,[a] Mario Monteiro,[a,†] Jianjun Li,[a] Mario Jacques,[b] Malcolm B. Perry[a] and Andrew D. Cox[a,*]

[a]*Institute for Biological Sciences, National Research Council, 100 Sussex Drive, Ottawa, ON, Canada K1A 0R6*
[b]*Faculté de médecine vétérinaire, Université de Montréal, St-Hyacinthe, Québec, Canada J2S-7C6*

Received 26 January 2004; accepted 29 April 2004
Available online 11 June 2004

**Abstract**—The structures of the core oligosaccharides of the lipopolysaccharides (LPS) from *Actinobacillus pleuropneumoniae* serotypes 1, 2, 5a and 5b were elucidated. The LPS's were subjected to a variety of degradative procedures. The structures of the purified products were established by monosaccharide and methylation analyses, NMR spectroscopy and mass spectrometry. The following structures for the core oligosaccharides were determined on the basis of the combined data from these experiments.

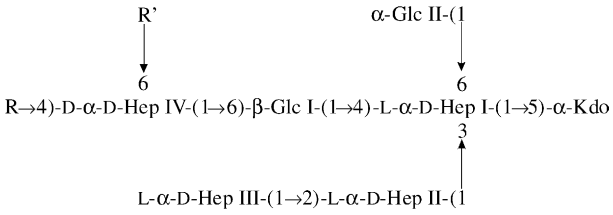


For serotype 1: R is (1*S*)-Gal*a*NAc-(1 → 4,6)-α-Gal II-(1 → 3)-β-Gal I-(1 →, and R′ is H
For serotype 2: R is β-Glc III-(1 →, and R′ is D-α-D-Hep V-(1 →
For serotypes 5a and 5b: R is H and R′ is D-α-D-Hep V-(1 →
All oligosaccharides elaborated a conserved inner core structure, as illustrated. All sugars were in the pyranose ring form apart from the open-chain *N*-acetylgalactosamine, the identification of which in the serotype 1 LPS was of interest.


*Keywords*: *Actinobacillus pleuropneumoniae*; LPS; Core oligosaccharide; Mass spectrometry; NMR

## 1. Introduction

*Actinobacillus pleuropneumoniae* (*Ap*) is a highly contagious respiratory porcine pathogen.[1] It is the causative agent of porcine fibrinohemorrhagic necrotising pleuropneumonia of widespread geographical incidence and of increasing economic importance as the trend towards confinement and intensified production of pigs continues.[1] The disease is highly contagious and causes tremendous economic loss to the swine industry.[1] Several virulence factors have been suggested, including the hemolytic and cytotoxic Apx toxins,[2] the polysaccharide capsule (CPS), some outer membrane proteins and lipopolysaccharide (LPS).[3,4] Fifteen serotypes of *Ap* have been identified.[5] The structural basis for the

* Corresponding author. Tel.: +1-613-991-6172; fax: +1-613-952-9092; e-mail: andrew.cox@nrc-cnrc.gc.ca
† Current address: Department of Chemistry and Biochemistry, University of Guelph, Guelph, ON, Canada N1G 2W1.

0008-6215/$ - see front matter © 2004 Elsevier Ltd. All rights reserved.
doi:10.1016/j.carres.2004.04.019

serology was shown to be the capsular polysaccharides and O-antigens of the LPS, which revealed that a specific LPS antigenic O-chain component was always associated with a specific CPS.[6] The LPS molecules contain lipid A, core oligosaccharide (OS) and O-antigenic polymers. The major adhesion has been identified as the LPS, which is involved in adherence to host respiratory cells.[7] The OS and not the lipid A region has been shown to be responsible for binding of *Ap* to porcine respiratory tract cells and mucus.[8] Additionally, deletions of the O-chain region of *Ap* have had no apparent effect on adherence, while an intact OS region appears to be required.[9]

SDS-PAGE studies have suggested that there are two OS types, I and II.[10] The purpose of our study was to determine the structure of the OS region from representatives of the OS type I; serotype 1, and OS type II; serotypes 2 and 5a. The genomic strain serotype 5b of OS type II was also investigated in order to assist subsequent studies towards an understanding of the genetic control of LPS biosynthesis.

## 2. Results

### 2.1. Investigation of *A. pleuropneumoniae* serotype 5a

Sugar analysis of the column-fractionated LPS revealed glucose (Glc), galactose (Gal), *N*-acetyl-glucosamine (GlcNAc), D-*glycero*-D-*manno*-heptose (DD-Hep) and L-*glycero*-D-*manno*-heptose (LD-Hep) in the approximate ratio of 2:1.5:1:2:3, respectively. GLC analysis of the derived butylglycosides revealed Glc and Gal to be D-isomers. The core OS was purified by gel-filtration chromatography of the acid hydrolysate. By examination of the elution profile, a fraction eluting at a volume consistent with core OS free from polymeric O-antigen was obtained and subjected to sugar analysis, which revealed the following: Glc, Gal, DD-Hep and LD-Hep in a ratio of 2:tr:2:3, respectively. As the capsular polysaccharide of serotype 5a contains *N*-acetyl-D-glucosamine and a ketose residue,[11] we suspected that the LPS had some capsule (CPS) contamination and that the fractionated core OS sample was devoid of CPS due to the sensitivity of the ketosidic bond in the CPS to the acid hydrolysis conditions employed to obtain the core OS. Additionally, the small amount of galactose in the core OS sample, the only O-antigen residue, suggested that the fraction examined was primarily core OS without significant O-antigen extension.

O-Deacylated LPS (LPS-OH) was prepared and fractionated by gel filtration chromatography. A fraction eluting at a volume consistent with containing a low proportion of O-antigen was analysed by CE-ESIMS (Table 1). A simple mass spectrum was observed corresponding to a molecule of 2537 amu, which is consistent with a composition of 2Hex, 5Hep, Kdo, P, Lipid A-OH. CE–MS/MS analysis (data not shown) on the doubly charged ion, $m/z$ 1268, gave two singly charged peaks at $m/z$ 951 and 1584, confirming the size of the O-deacylated lipid A as 952 amu and the core OS as 1584. The O-deacylated lipid A species (952 amu) consists of a disaccharide of N-acylated (3-OH:C 14:0) glucosamine residues, each residue being substituted with a phosphate molecule. ESIMS and CE-ESIMS analyses of the fractionated OS sample revealed a mass of 1505 Da, consistent with a composition of 2Hex, 5Hep, Kdo (Table 1). The CE-ESIMS spectrum of a later eluting core OS fraction had a mass of 1562, 57 amu higher than the major glycoform (Table 1). This mass corresponds to the amino acid glycine as has been recently observed in the LPS of *Neisseria meningitidis* and *Haemophilus*

**Table 1.** Negative-ion ESIMS and CE-ESIMS data and proposed compositions of O-deacylated LPS and core oligosaccharides from *A. pleuropneumoniae* serotypes 1, 2, 5a and 5b

| Serotype | Observed ions ($m/z$) | | Molecular mass (Da) | | Proposed composition |
|---|---|---|---|---|---|
| | $(M-2H)^{2-}$ | $(M-3H)^{3-}$ | Observed | Calculated | |
| 1 O-deac | 1396 | 930 | 2794 | 2792.7 | HexNAc, 4Hex, 4Hep, Kdo, Lipid A-OH |
| | 1436 | 957 | 2874 | 2872.6 | HexNAc, 4Hex, 4Hep, Kdo, P, Lipid A-OH |
| | 1497 | 998 | 2997 | 2995.7 | HexNAc, 4Hex, 4Hep, Kdo, P, PEtn, Lipid A-OH |
| Core OS | 919 | — | 1840 | 1840.7 | HexNAc, 4Hex, 4Hep, aKdo[a] |
| | 928 | | 1858 | 1858.7 | HexNAc, 4Hex, 4Hep, Kdo |
| 2 O-deac | 1309 | 872 | 2620 | 2620.5 | 3Hex, 5Hep, Kdo, Lipid A-OH |
| | 1349 | 899 | 2700 | 2699.5 | 3Hex, 5Hep, Kdo, P, Lipid A-OH |
| Core OS | 832 | — | 1667 | 1667.5 | 3Hex, 5Hep, Kdo |
| 5a and 5b O-deac | 1268 | 845 | 2537 | 2537.4 | 2Hex, 5Hep, Kdo, P, Lipid A-OH |
| Core OS | 752 | | 1505 | 1505.3 | 2Hex, 5Hep, Kdo |
| | 780 | | 1562 | 1562.3 | 2Hex, 5Hep, Kdo, Gly |

Average mass units were used for calculation of molecular weight based on proposed composition as follows: Hex, 162.15; HexNAc, 203.19; Hep, 192.17; Kdo, 220.18; P, 79.98; PEtn, 123.05; Gly, 57.05. O-deacylated lipid A (Lipid A-OH) is 952.00.

[a]The major ion corresponded to the molecular ion – 18 (loss of $H_2O$).

*influenzae*.[12,13] CE-ESIMS/MS analyses located this glycine residue on the second heptose residue (Hep II) from the Kdo molecule (data not shown).

Methylation analysis was performed on the core OS in order to determine the linkage pattern of the molecule. Analysis on a fraction corresponding to core OS alone revealed the presence of approximately equimolar amounts of terminal Glc, 6-substituted Glc, terminal DD-Hep, terminal LD-Hep, 6-subsituted DD-Hep, 2-substituted LD-Hep and 3,4,6-tri-substituted LD-Hep. It was possible to discriminate between the LD- and DD-heptose isomers by GC–MS of the partially methylated alditol acetates (PMAA) by comparison to existing PMAA samples in the laboratory from published data on *Mannheimia haemolytica*[14] and *H. influenzae*.[15] Analysis of an earlier fraction of the OS, containing predominantly O-antigen, revealed the presence of 6-substituted Gal (the O-antigenic component) confirming the linkage pattern of the O-antigen.[6]

In order to elucidate the exact locations and linkage patterns of the OS, NMR studies were performed on the OS fraction enriched for the absence of O-antigen (Fig. 1a). The assignment of $^{1}$H-resonances of the OS was achieved by COSY and TOCSY experiments. Full assignment of both $^{13}$C- and $^{1}$H-resonances was completed following $^{13}$C–$^{1}$H HSQC, $^{13}$C–$^{1}$H HSQC-TOCSY and $^{13}$C–$^{1}$H HMBC experiments. Figure 2 shows a series of selective 1D-TOCSY experiments from the anomeric $^{1}$H resonance of each residue in the OS. In the course of the NMR analysis, it became apparent that the *Ap* 5a OS was structurally related to the recently published structure of *M. haemolytica* core OS,[14] and assignment of the *Ap* 5a OS spectra was aided by reference to this $^{1}$H NMR data (Table 2).

In the selective spectra of the *Ap* 5a OS, spin systems arising from heptose residues (Fig. 2a–e) were readily

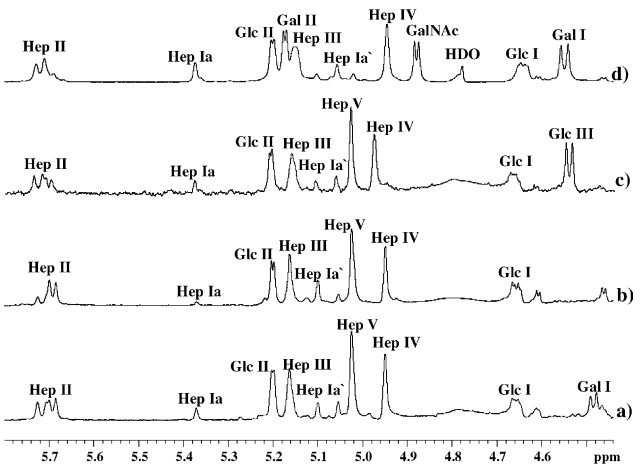


**Figure 1.** Anomeric regions of the $^{1}$H NMR spectra of the core OS from *Ap* serotypes (a) 5a; (b) 5b; (c) 2; (d) 1. The spectra were recorded in $D_2O$ at pH 7.0 and 25 °C. A small amount of O-chain β-galactose was observed in serotype 5a.

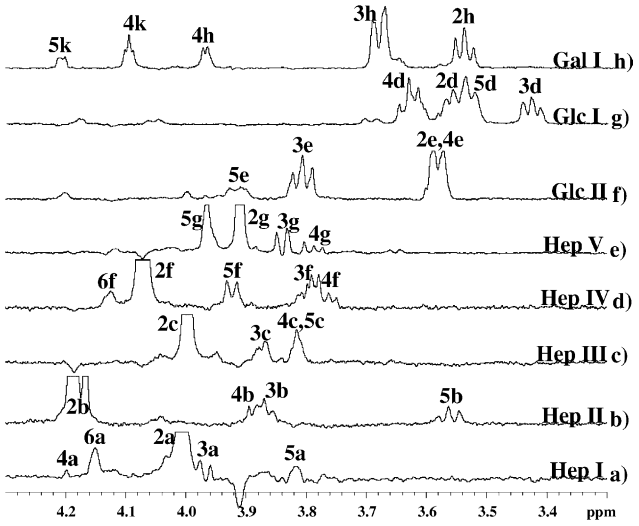


**Figure 2.** Ring regions of the selective 1D-TOCSY NMR spectra of the core OS from *Ap* serotype 5a residues (a) Hep I; (b) Hep II; (c) Hep III; (d) Hep IV; (e) Hep V; (f) Glc II; (g) Glc I; (h) Gal I. Letter designations for each residue are as indicated in Table 2. The spectra were recorded in $D_2O$ at pH 7.0 and 25 °C with mixing times of 150 ms for the heptose residues and 90 ms for the hexose residues.

identified from their anomeric $^{1}$H-resonances at 5.11 (Hep I, a), 5.70 (Hep II, b), 5.17 (Hep III, c), 4.96 (Hep IV, f) and 5.03 (Hep V, g) ppm, coupled with the appearance of their spin systems that pointed to *manno*-pyranosyl ring systems. Complete assignment enabled discrimination between DD- and LD-Hep residues by virtue of the $^{13}$C-resonance for the C-6 carbons for Hep II, Hep III and Hep V.[16] Hep I and Hep IV were assigned by comparison to published data from the OS of *M. haemolytica*.[14] The heterogeneity observed for the anomeric protons of Hep I and Hep II (Fig. 1a) was due to rearrangements of the Kdo residue on acid hydrolysis. Examination of the $^{1}$H NMR spectrum of completely deacylated LPS revealed a 1:1 ratio for the anomeric resonances of these residues (data not shown). The remaining residue in the α-anomeric region at 5.21 ppm (Glc II, e) was determined to be *gluco*-pyranose sugar, based upon the appearance of its spin system (Fig. 2f). The remainder of the anomeric resonances in the β-region (4.45–5.00 ppm) of the spectrum were all attributable to β-linked residues by virtue of their anomeric $^{1}$H-resonances and in the case of resolved residues their high $J_{1,2}$ (~8 Hz) coupling constants. One of the resonances at 4.66 ppm (Glc I, d) was assigned to the *gluco*-configuration from the appearance of the spin system (Fig. 2g). The remaining resonance in the low-field region at 4.49 (Gal I, h) ppm was assigned to a *galacto*-pyranosyl residue from the appearance of the characteristic spin system to the H-4 resonance in a TOCSY experiment (Fig. 2h). The Kdo spin system was also accessed in this experiment as the H-6 $^{1}$H-resonance of Kdo at 4.48 ppm was also irradiated and revealed the

**Table 2.** $^{1}H$ and $^{13}C$ NMR chemical shifts for the core OS from *A. pleuropneumoniae* serotypes 1, 2, 5a and 5b

| | H-1 | H-2 | H-3 | H-4 | H-5 | H-6 | H-7 | NOEs | | |
|---|---|---|---|---|---|---|---|---|---|---|
| | | | | | | | | Inter | Intra | Long range |
| *Inner core*[a] | | | | | | | | | | |
| Serotypes 1, 2, 5a, 5b | | | | | | | | | | |
| Kdo | — | — | 2.08 | 4.10 | 4.21 | 4.48 | nd | | | |
| (k) | | | 1.92 | | | | | | | |
| Hep-I | 5.11 | 4.01 | 3.97 | 4.21 | 3.82 | 4.15 | 3.88 | 4.20 Kdo H-5 | 4.01 H-2 | |
| (a) | (98.9) | (71.2) | (73.7) | (74.7) | (72.6) | (80.3) | 3.73 | | | |
| | | | | | | | (62.9) | | | |
| Hep-I | 5.37 | 4.08 | 3.95 | 4.22 | 3.78 | 4.13 | 3.88 | nd | 4.08 H-2 | |
| (a′) | (101.3) | (71.2) | (73.5) | (74.6) | (72.6) | (80.3) | 3.73 | | | |
| | | | | | | | (62.9) | | | |
| Hep-II | 5.70 | 4.19 | 3.87 | 3.89 | 3.55 | 4.04 | 3.76 | 5.15 Hep III H-1 | 4.19 H-2 | 3.82 Hep I H-5 |
| (b) | (100.2) | (80.5) | (70.7) | (67.5) | (72.7) | (70.3) | 3.74 | 3.97 Hep I H-3 | 3.87 H-3 | 3.82 Hep III H-5 |
| | | | | | | | (64.2) | | | 3.77 Hep III H-7a |
| | | | | | | | | | | 3.56 Glc I H-2 |
| Hep-III[b] | 5.17 | 4.00 | 3.88 | 3.82 | 3.82 | 4.06 | 3.93 | 5.70 Hep II H-1 | 4.00 H-2 | 4.08 Hep IV H-2 |
| (c) | (102.3) | (71.5) | (71.6) | (67.1) | (72.4) | (70.2) | 3.93 | 4.19 Hep II H-2 | | 3.80 Hep IV H-3 |
| | | | | | | | (70.3) | | | 3.63 Glc I H-4 |
| Hep-III[c] | 5.17 | 4.00 | 3.88 | 3.82 | 3.82 | 4.04 | 3.77 | 5.70 Hep II H-1 | 4.00 H-2 | 4.08 Hep IV H-2 |
| (c) | (102.3) | (71.5) | (71.6) | (67.1) | (72.4) | (70.2) | 3.62 | 4.19 Hep II H-2 | | 3.80 Hep IV H-3 |
| | | | | | | | (64.6) | | | 3.63 Glc I H-4 |
| β-Glc (Glc-I) | 4.66 | 3.56 | 3.43 | 3.63 | 3.54 | 4.06 | — | 4.21 Hep I H-4 | 3.54 H-5 | 5.21 Glc II H-1 |
| (d) | (104.0) | (74.1) | (77.8) | (70.3) | (74.5) | 3.70 | | 4.15 Hep I H-6 | 3.43 H-3 | |
| | | | | | | (65.5) | | | | |
| α-Glc (Glc-II) | 5.21 | 3.58 | 3.81 | 3.59 | 3.92 | 3.96 | — | 4.15 Hep I H-6 | 3.58 H-2 | 4.66 Glc I H-1 |
| (e) | (102.6) | (72.8) | (73.8) | (69.3) | (72.4) | 3.76 | | | | |
| | | | | | | (60.2) | | | | |
| *Outer core* | | | | | | | | | | |
| Serotypes 5a, 5b | | | | | | | | | | |
| Hep-IV | 4.96 | 4.08 | 3.80 | 3.78 | 3.93 | 4.13 | 3.90 | 4.06 Glc I H-6a | 4.08 H-2 | |
| (f) | (99.8) | (70.5) | (71.7) | (68.1) | (71.9) | (77.0) | 3.80 | 3.70 Glc I H-6b | | |
| | | | | | | | (61.2) | | | |
| Hep-V | 5.03 | 3.92 | 3.84 | 3.79 | 3.97 | 4.02 | 3.79 | 4.13 Hep IV H-6 | 3.92 H-2 | 4.19 Hep II H-2 |
| (g) | (99.0) | (70.8) | (71.5) | (68.2) | (73.7) | (73.1) | 3.74 | 3.93 Hep IV H-5 | 3.97 H-5 | 4.04 Hep II H-6 |
| | | | | | | | (63.0) | | | 3.93 Hep IV H-5 |
| β-Gal (Gal-I) | 4.49 | 3.55 | 3.68 | 3.97 | 3.93 | 3.75 | — | 3.93 Hep III H-7a | 3.68 H-3 | |
| (h) | (104.2) | (71.6) | (73.4) | (69.5) | (74.5) | 3.61 | | 3.93 Hep III H-7b | 3.93 H-5 | |
| | | | | | | (65.7) | | | | |
| Serotype 2 | | | | | | | | | | |
| Hep-IV | 4.96 | 4.13 | 3.90 | 3.96 | 4.05 | 4.30 | 3.97 | 4.06 Glc I H-6a | 4.14 H-2 | |
| | (99.5) | (70.3) | (70.6) | (78.0) | (70.3) | (75.4) | 3.82 | 3.70 Glc I H-6b | | |
| | | | | | | | (60.9) | | | |
| Hep-V | 5.02 | 3.88 | 3.82 | 3.78 | 3.97 | 4.00 | 3.80 | 4.30 Hep IV H-6 | 3.88 H-2 | |
| | (98.6) | (70.7) | (71.5) | (68.1) | (73.9) | (73.0) | 3.74 | 4.05 Hep IV H-5 | | |
| | | | | | | | (62.8) | | | |
| β-Glc (Glc III) | 4.53 | 3.33 | 3.51 | 3.41 | 3.51 | 3.95 | — | 3.96 Hep IV H-4 | 3.51 H-3 | |
| | (103.4) | (74.0) | (76.4) | (70.4) | (77.0) | 3.74 | | 4.30 Hep IV H-6 | 3.51 H-5 | |
| | | | | | | (61.6) | | 4.05 Hep IV H-5 | | |
| Serotype 1 | | | | | | | | | | |
| Hep-IV[d] | 4.95 | 4.13 | 3.94 | 3.94 | 3.94 | 3.78 | 3.83 | 4.15 Glc I H-6a | 4.13 H-2 | |
| (m) | (99.7) | (70.2) | (70.7) | (79.5) | (72.9) | (76.1) | 3.80 | 3.74 Glc I H-6b | | |
| | | | | | | | (61.9) | | | |
| β-Gal (Gal-I) | 4.55 | 3.67 | 3.79 | 4.17 | 4.17 | 3.87 | — | 3.94 Hep IV H-4 | 3.79 H-3 | |
| (l) | (103.9) | (70.3) | (78.4) | (65.9) | (71.6) | 3.75 | | | 4.17 H-5 | |
| | | | | | | (62.4) | | | | |
| α-Gal (Gal-II) | 5.18 | 3.97 | 4.06 | 4.25 | 4.13 | 4.12 | — | 3.79 Gal I H-3 | 3.97 H-2 | |
| (j) | (97.3) | (68.8) | (68.7) | (76.7) | (64.2) | 4.01 | | | | |
| | | | | | | (69.5) | | | | |
| (1*S*)-Gal*a* NAc | 4.88 | 4.34 | 4.13 | 3.36 | 3.93 | 3.66 | — | 4.25 Gal II H-4 | 4.34 H-2 | |
| (i) | (101.1) | (52.6) | (68.5) | (70.0) | (70.7) | 3.64 | | 4.12 Gal II H-6a | | |
| | | | | | | (64.1) | | 4.01 Gal II H-6b | | |

Chemical shifts are given in ppm relative to internal acetone at 2.225 and 31.07 ppm. Letter designation used for residues in figures is as indicated in parentheses. [a]Inner core data derived from serotype 5a. Chemical shifts from other serotypes inner core residues were virtually identical. [b]Data for substituted Hep III residue in serotypes 5a and 5b. [c]Data for terminal Hep III residue of serotypes 1 and 2. [d]For serotype 1, $^{1}H$-resonances for Glc I H-6a and H-6b are 4.15 and 3.74 ppm, respectively.

H-4 and H-5 $^{1}$H-resonances at 4.10 and 4.21 ppm, respectively. However, the spin system of Kdo was difficult to completely determine due to rearrangements of the Kdo residue on core hydrolysis and the very low-intensity levels of the methylene H-3 protons, which were probably due to deuterium exchange. However, the spin system was further assigned in another 1D-TOCSY experiment from the H-3 axial proton at 1.92 ppm, revealing $^{1}$H-resonances for the equatorial proton at 2.08 ppm and the H-4 proton at 4.10 ppm (data not shown).

The sequence of the glycosyl residues in the OS was determined from the interresidue $^{1}$H–$^{1}$H NOE measurements between anomeric and aglyconic protons on adjacent glycosyl residues, confirming and extending the methylation analysis data. The linkage pattern for the *Ap* 5a OS was determined in this way (Fig. 3) (Table 2). Thus the occurrence of intense transglycosidic NOE connectivities between the proton pairs Hep III H-1 and Hep II H-2 and Hep II H-1 and Hep I H-3 established the sequence and points of attachment of the three LD-heptose residues. This linkage pattern is commonly encountered in the inner core OS from *M. haemolytica* and *H. influenzae*.[14,15] Furthermore, interresidue NOE's between the anomeric protons Hep III H-1 and Hep II H-1 (data not shown) provided confirmation of the $(1\rightarrow 2)$-linkage.[17] Examination of NOE connectivities from H-1 of Glc I illustrated that this glucose residue was connected to Hep I at the 4-position by virtue of interresidue NOE's to Hep I H-4 and Hep I H-6. The appearance of an interresidue NOE to H-6 is a common occurrence for 4-substituted heptose residues.[18] The occurrence of a long-range NOE connectivity between H-1 of Glc I and H-1 of Glc II suggested that the α-configured glucose residue (Glc II) was substituting Hep I at the 6-position as has been observed previously for the OS from *M. haemolytica*.[14] The similarity between the OS from *M. haemolytica* and *Ap* was evident from other similar long-range NOE connectivities (Fig. 3) observed in *Ap* suggesting that the two core OS molecules had similar conformations.[14] Examination of NOE connectivities from H-1 of Glc II confirmed that this glucose residue was connected to Hep I at the 6-position by virtue of interresidue NOE's to Hep I H-6. The linkage positions of the remaining heptose residues (Hep IV and Hep V) were deduced as follows. Examination of NOE connectivities from H-1 of Hep IV revealed that this heptose residue was connected to Glc I at the 6-position by virtue of interresidue NOE's to Glc I H-6 and H-6′. Finally, Hep V was determined to be substituting Hep IV at the 6-position by virtue of a NOE connectivity from Hep V H-1 to Hep IV H-6. A $^{13}$C–$^{1}$H HMBC experiment was performed in order to confirm the linkage pattern of the core OS, and for the majority of linkages, a correlation was observed between the anomeric $^{1}$H-resonance and the $^{13}$C-resonance at the point of attachment, thus confirming the NOE connectivities and methylation data. In this way it was possible to confirm that the Glc I residue substituted Hep I at the 4-position, and the Glc II residue substituted Hep I at the 6-position (data not shown and similar data for serotype 1 (Fig. 7)). Additionally, NMR analysis of OS from serotype 5a enabled the point of attachment of the O-chain galactose residue to be identified. A fraction that contained just one galactose residue was utilised for this purpose. NOE connectivities from the anomeric $^{1}$H-resonance included intra-connectivities to H-3 and H-5 at 3.68 and 3.93 ppm and an inter-connectivity to 3.93 ppm (Fig. 4a). Selective 1D experiments were then utilised to identify the spin-system of the proton resonance at 3.93 ppm. A 1D-NOESY–TOCSY experiment from the H-1 proton of Gal I in the NOESY step, followed by selective excitation of the resonance at 3.93 ppm in the TOCSY step, confirmed the connectivity of the resonance at 3.93 ppm to a resonance at 4.06 ppm (Fig. 4b). A 1D-TOCSY experiment from the anomeric proton resonance of the Hep III residue at 5.17 ppm utilising a 150 ms mixing time revealed the H-4 and H-5 proton resonances of this spin-system at 3.82 ppm (Fig. 2c). This resonance was then selectively irradiated in a NOESY step that revealed the Hep III H-6 resonance at 4.06 ppm, thus confirming the 7-position of the Hep III residue as the point of attachment of the O-chain (Fig. 4c). Confirmatory data was obtained from a $^{13}$C–$^{1}$H HMBC experiment that identified a cross-peak from the anomeric $^{1}$H-resonance of the O-chain galactose residue at 4.49 ppm that correlated with a $^{13}$C-resonance at 70.3 ppm (Fig. 5d), which in a $^{13}$C–$^{1}$H HSQC

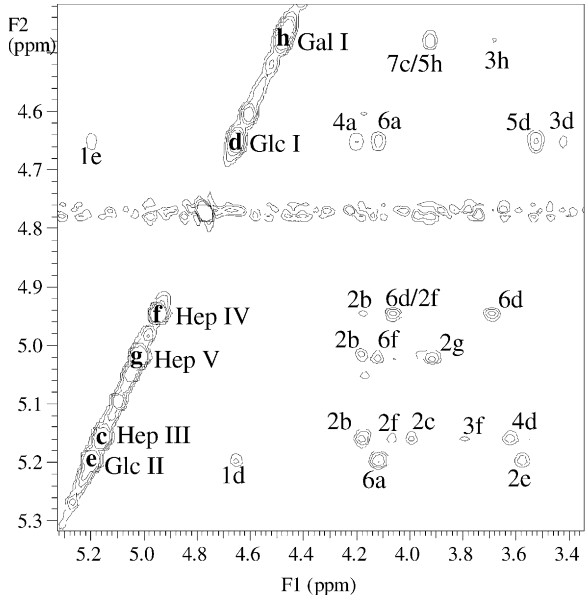


**Figure 3.** Region of the 2D-NOESY NMR spectrum of the core OS from *Ap* serotype 5a. Letter designations for each residue are as indicated in Table 2. The spectrum was recorded in $D_2O$ at pH 7.0 and 25 °C with a mixing time of 400 ms.

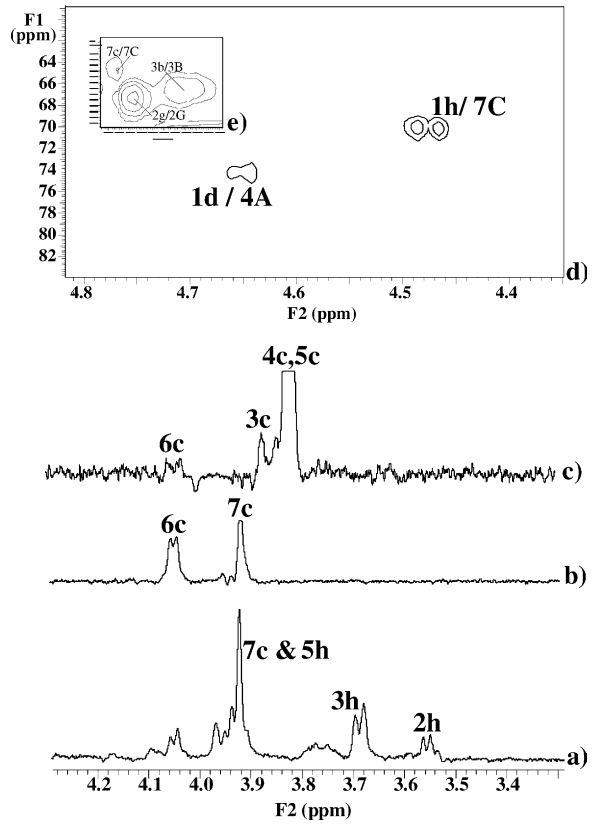


**Figure 4.** Determination of the location of the O-chain Gal I residue of the core OS from *Ap* serotype 5a. (a) 1D-NOESY NMR spectrum from the anomeric $^{1}$H-resonance of Gal I; (b) 1D-NOESY–TOCSY spectrum from the anomeric $^{1}$H-resonance of Gal I residue in the NOESY step and from the H-7 $^{1}$H-resonance of the Hep III residue in the TOCSY step; (c) 1D-TOCSY–NOESY spectrum from the anomeric $^{1}$H-resonance of Hep III residue in the TOCSY step and from the H-4/H-5 $^{1}$H-resonances of the Hep III residue in the NOESY step. (d) Region of the $^{13}$C–$^{1}$H-HMBC NMR spectrum indicating the HMBC from the anomeric $^{1}$H-resonances of Gal I and Glc I. (e) Region of the $^{13}$C–$^{1}$H-HSQC NMR spectrum indicating the $^{13}$C-cross-peaks from the H-7 $^{1}$H-resonance of Hep III, the H-2 $^{1}$H-resonance of Hep V and the H-3 $^{1}$H-resonance of Hep II. The spectra were recorded in $D_2O$ at pH 7.0 and 25 °C.

experiment was found to correlate to the proton resonance at 3.93 ppm (Fig. 4e), which appeared as positive peak in a $^{13}$C–$^{1}$H HSQC spectrum indicative of a $-CH_2-$ group, confirming the 7-position of a heptose residue as the point of O-chain attachment. This conclusion was confirmed by methylation analysis on a fraction that contained just one galactose residue that indicated the presence of a 7-substituted LD-Hep residue; this permethylated alditol acetate derivate was not observed following methylation analysis of a core OS fraction devoid of O-chain.

### 2.2. Investigation of *A. pleuropneumoniae* serotype 5b

All analyses of LPS, LPS-OH and OS from serotype 5b were identical or very similar to the previous analyses described for serotype 5a (Tables 1 and 2; Fig. 1b).

### 2.3. Investigation of *A. pleuropneumoniae* serotype 2

Sugar analysis of the intact LPS revealed the presence of Glc, DD-Hep, LD-Hep, Rha, Gal, GlcNAc and GalNAc in the approximate ratio 8:2:2:1:2:1:2, which is consistent with the presence of O-antigen and capsular polysaccharide in this material.[19,20] Sugar analysis of the fractionated acid hydrolysate revealed the presence of Glc, Rha, Gal and GalNAc in an early eluting fraction, in the approximate ratio of 2:1:1:1 that is consistent with a fraction enriched for O-antigen. A later fraction enriched for the absence of O-antigen revealed the presence of only Glc, DD-Hep and LD-Hep in the approximate ratio of 3:2:3 consistent with the absence of O-antigen from this core OS fraction. GLC analysis of the derived *sec*-butylglycosides revealed Glc to be in the D-configuration.

LPS-OH was prepared and fractionated by gel, filtration chromatography. A fraction eluting at a volume consistent with containing a low proportion of O-antigen was analysed by CE-ESIMS in the negative-ion mode (Table 1). A simple mass spectrum was observed corresponding to a molecule of 2700 amu that is consistent with a composition of 3Hex, 5Hep, Kdo, P, Lipid A-OH with minor amounts of a second molecule indicated with a mass of 80 amu lower, consistent with the absence of a phosphate residue. CE-MS/MS analysis (data not shown) on the triply charged ion $m/z$ 899 gave a singly charged peak at $m/z$ 951, confirming the size of the O-deacylated lipid A as 952 amu for the major molecule of mass 2700 amu. CE-ESIMS analyses of the fractionated core OS sample enriched for absence of the O-antigen revealed a mass of 1667 Da, consistent with a composition of 3Hex, 5Hep, Kdo (Table 1). Mass spectrometric analyses therefore indicated that the core OS of serotype 2 contained an additional glucose residue than the core OS from serotypes 5a and 5b.

Methylation analysis of the core OS fraction enriched for absence of O-antigen revealed the presence of terminal Glc, 6-substituted Glc, terminal DD-Hep, terminal LD-Hep, 2-substituted DD-Hep, 2-substituted LD-Hep, 4,6-di-subsituted DD-Hep and 3,4,6-tri-substituted LD-Hep in the approximate ratio 6:3:3:2:tr:2:3:2. Similar to the PMAA analysis of serotypes 5a and b, the assignment of the heptose residues was based on comparison to previously published data.[14,15] In the case of the 4,6-DD-Hep, this assignment was confirmed by comparison with a *Pasteurella multocida* LPS sample that only contained LD-Hep residues, and following PMAA analysis, a 4,6-LD-Hep was identified that resolved from the *Ap* serotype 2 4,6-Hep signal (unpublished data). The main discrepancy between the methylation data for the serotype 2 and 5b OS was the replacement of the mono-6-substituted DD-Hep, with a 4,6-di-substituted DD-Hep, tentatively identifying the 4-position of the internal DD-Hep residue as the point of attachment of

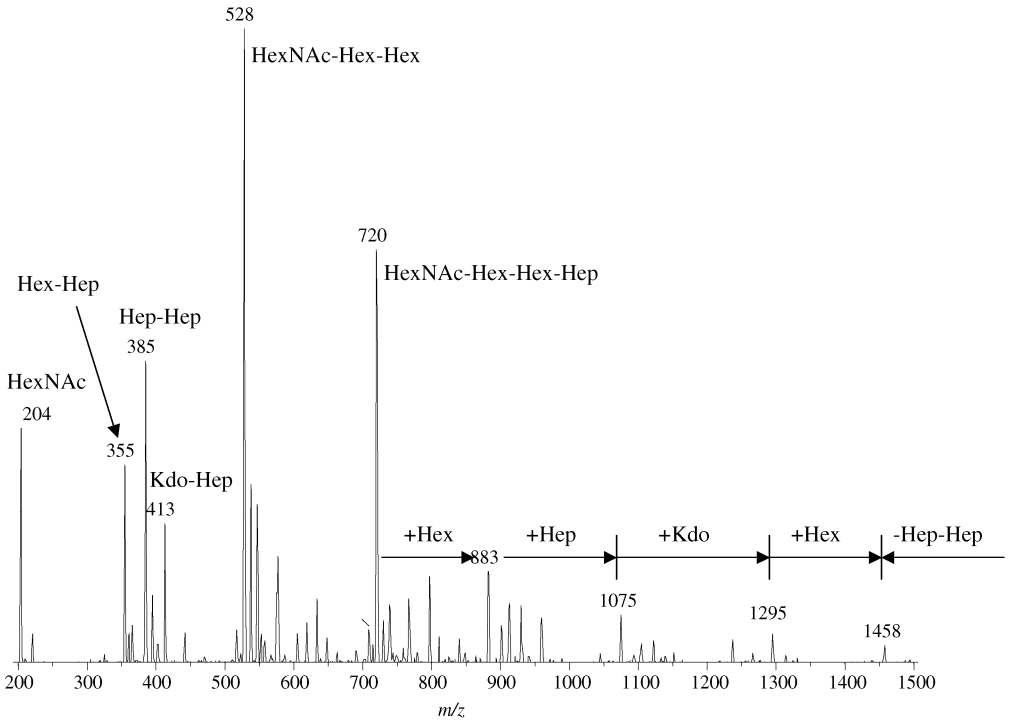


**Figure 5.** Positive ion capillary electrophoresis-electrospray mass spectrum of the core OS from *Ap* serotype 1. Product ion spectrum from $m/z$ $930^{2+}$.

the additional glucose residue. The ratio of terminal glucose residues, identified by methylation analyses, between serotypes 2 and 5b is also consistent with the presence of an additional terminal glucose residue in the core OS of serotype 2.

$^{1}$H NMR data (Table 2; Fig. 1c) corroborated the mass spectrometric and methylation analyses data, confirming that the core OS of serotype 2 was identical to that found for serotypes 5a and b, but with the identification of an additional terminal β-configured glucose residue (Glc III). NOE data defined the point of attachment of the Glc III residue at the 4-position of Hep IV by virtue of an inter-NOE connectivity from the $^{1}$H-resonance of the anomeric proton of Glc III at 4.53 ppm to the $^{1}$H-resonance of the 4-position of Hep IV at 3.96 ppm (data not shown). A NOE connectivity was also observed to the 6-position of Hep IV as has been observed previously for 4-substituted heptose residues. A $^{13}$C–$^{1}$H HMBC experiment was performed in order to confirm the linkage between the Glc III and Hep IV residues. In this way it was possible to confirm that the Glc III residue substituted Hep IV at the 4-position and the Hep V residue substituted Hep IV at the 6-position (data not shown).

### 2.4. Investigation of *A. pleuropneumoniae* serotype 1

Sugar analysis of the column-fractionated LPS revealed the presence of Rha, Glc, Gal, GlcNAc, DD-Hep and LD-Hep in an approximate ratio of 1:3:1:0.5:1:3. The identification of Rha and GlcNAc suggested some O-antigenic components were still present in this fraction.[20] Sugar analysis of a core OS fraction enriched for absence of O-antigen revealed Glc, Gal, DD-Hep and LD-Hep in the ratio 2:1.5:1:3. GLC analysis of the derived *sec*-butylglycosides revealed Glc and Gal to be D-isomers. Sugar analysis on earlier fractions containing full length O-antigen revealed Rha, Glc and GlcNAc in an approximate ratio of 2:1:1, consistent with the published structure for the O-antigen of this serotype.[21]

LPS-OH was prepared and fractionated by gel-filtration chromatography. A fraction eluting at a volume consistent with containing a low proportion of O-antigen was analysed by ESIMS and CE-ESIMS in the negative ion mode (Table 1). A simple mass spectrum was observed corresponding to a molecule of 2874 amu consistent with a composition of 4Hex, HexNAc, 4Hep, Kdo, P, Lipid A-OH with minor amounts of a second molecule indicated with a mass of 123 amu higher, consistent with the presence of an additional phosphoethanolamine residue and a third molecule with a mass of 80 amu lower, consistent with the absence of a phosphate residue. CE–MS/MS analysis (data not shown) on the triply charged ion $m/z$ 957, gave a singly charged peak at $m/z$ 951 confirming the size of the O-deacylated lipid A as 952 amu for the major molecule of mass 2874 amu and a doubly charged ion at $m/z$ 959 corresponding to the core OS. ESIMS and CE-ESIMS analyses on several core OS fractions enriched for

absence of the O-antigen revealed a mass of 1840 Da, consistent with a composition of 4Hex, HexNAc, 4Hep, Kdo (Table 1). CE–MS/MS analysis in the positive-ion mode on the doubly charged ion at $m/z$ 930 that corresponds to the core OS was performed. Singly charged ions consistent with the presence of the following groups of residues in serotype 1 core OS were observed including, HexNAc $m/z$ 204, Hex-Hex-HexNAc $m/z$ 528, Hep-Hex-Hex-HexNAc $m/z$ 720 (Fig. 5). Mass spectrometric analyses therefore indicated that the core OS of serotype 1 contained one DD-Hep residue less than the core OS from serotypes 5a and 5b, but contained and an additional 2 Hex's and a HexNAc residue. However the absence of evidence for HexNAc in sugar analysis of core OS enriched for the absence of O-antigen was initially confusing.

Methylation analysis on a core OS fraction enriched for absence of O-antigen revealed the presence of terminal Glc, 6-substituted Glc, 3-substituted Gal, terminal LD-Hep, 4,6-disubstituted Gal, 4-subsituted DD-Hep, 2-substituted LD-Hep and 3,4,6-trisubstituted LD-Hep in approximately equimolar amounts. Discrimination between the LD and DD-Hep residues was achieved in the same way as for serotypes 2, 5a and b. Once again the absence of any evidence for a HexNAc residue was perplexing.

The mass spectrometric, sugar and methylation analyses data were therefore consistent with the inner core structure observed for serotypes 2, 5a and 5b, and $^1$H NMR data corroborated these inferences (Fig. 1d; Table 2). $^1$H NMR data also enabled identification of the additional core OS H-1 resonances not present in the core OS from serotypes 2, 5a and 5b. An α- and a β-configured galactose residues (Gal II, j and Gal I, l, respectively) were assigned with H-1 resonances of 5.18 and 4.55 ppm by virtue of characteristic spin systems to the H-4 $^1$H-resonances in a TOCSY experiment. An α-configured *N*-acetylhexosamine residue (HexNAc, i) was inferred with the H-1 resonance of 4.88 ppm by virtue of the $^1$H-resonance of its H-2 proton at 4.34 ppm correlating to a $^{13}$C chemical shift of 52.6 ppm in a $^{13}$C–$^1$H HSQC experiment (Fig. 6a). The $^{13}$C chemical shift was consistent with a nitrogen substituted carbon atom. However, it was very difficult to access the spin system of this HexNAc residue beyond the H-2 proton, and the chemical shift of the H-2 proton seemed to be of considerably low field. Interresidue NOE connectivities established the linkage pattern between the anomeric proton of the Gal I residue at 4.55 ppm and the 4-position of Hep IV at 3.94 ppm. In a similar way an NOE connectivity between the anomeric proton of the Gal II at 5.18 ppm and the 3-position of the Gal I residue at 3.79 ppm established this linkage. However, interresidue NOE connectivities between the anomeric proton of the HexNAc residue at 4.88 ppm and the 4-position of the Gal II residue at 4.25 ppm and the 6-position of this residue at 4.12 and 4.01 ppm suggested that the HexNAc residue was substituting the Gal II residue at both the 4- and 6-positions, consistent with the methylation analysis data but nonetheless confusing (Fig. 6c). FABMS of the methylated OS gave further insight into the sequence of the sugars of this portion of the OS. The $m/z$ of the A-type primary glycosyl oxonium ions and secondary ions (loss of methanol) observed were as follows, $464 \rightarrow 432$ $(Hex, HexNAc)^+$, $668 \rightarrow 636$ $(Hex_2, HexNAc)^+$, $916 \rightarrow 884$ $(Hex_2, HexNAc, Hep)^+$, $1120 \rightarrow 1088$ $(Hex_3, HexNAc, Hep)^+$, 1368 $(Hex_3, HexNAc, Hep_2)^+$, $1572 \rightarrow 1540$ $(Hex_4, HexNAc, Hep_2)^+$ and $1865 \rightarrow 1833$ $(Hex_3, HexNAc, Hep_4)^+$. This FAB data was consistent with the NOE and positive-ion CE–ESIMS/MS data, but the lack of evidence for a terminal HexNAc residue was confusing but in agreement with the sugar analysis and methylation analysis data. Further proof of the linkage pattern of the outer core region was obtained from a $^{13}$C–$^1$H-HMBC experiment (Fig. 7), which confirmed the NOE and methylation analysis data. The lack of definitive data for the HexNAc residue therefore

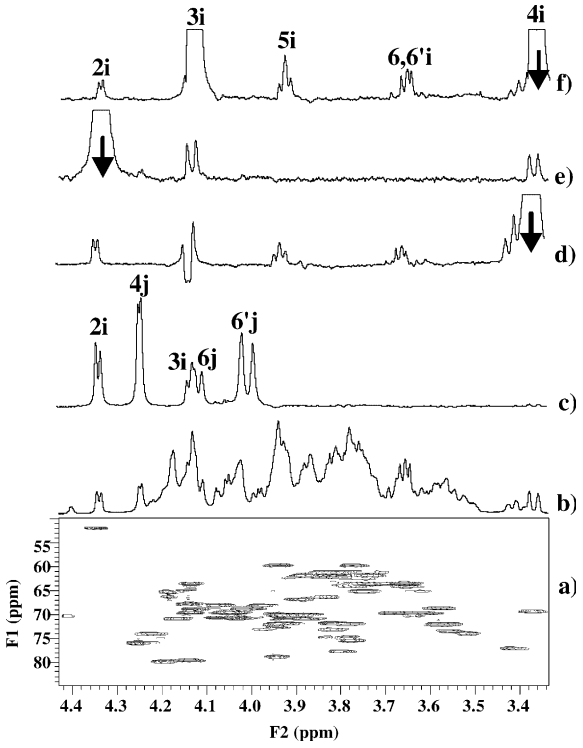


**Figure 6.** Identification of the open-chain *N*-acetylgalactosamine residue of the core OS from *Ap* serotype 1. (a) Ring region of the 2D-$^{13}$C–$^1$H-HSQC NMR spectrum of the core OS from *Ap* serotype 1. (b) Ring region of the $^1$H NMR spectrum of the core OS from *Ap* serotype 1. (c) 1D-NOESY spectrum from the H-1 $^1$H-resonance of the GalNAc residue. (d) 1D-TOCSY spectrum from the H-4 $^1$H-resonance of the GalNAc residue. (e) 1D-NOESY spectrum from the H-2 $^1$H-resonance of the GalNAc residue. (f) 1D-NOESY spectrum from the H-4 $^1$H-resonance of the HexNAc residue. The spectra were recorded in $D_2O$ at pH 7.0 and 25 °C. The assignments of the resonances are as indicated (i, GalNAc; j, Gal II).

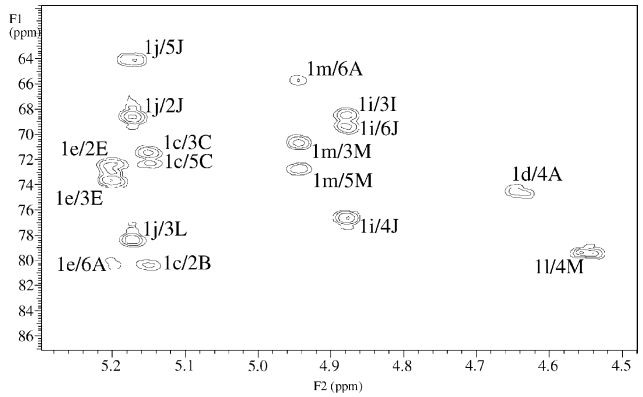


**Figure 7.** Region of the 2D-$^{13}$C–$^{1}$H-HMBC NMR spectrum of the core OS from *Ap* serotype 1 showing correlations between anomeric $^{1}$H-resonances (lower case letters) and ring $^{13}$C-resonances (upper case letters). The spectrum was recorded in $D_2O$ at pH 7.0 and 25 °C.

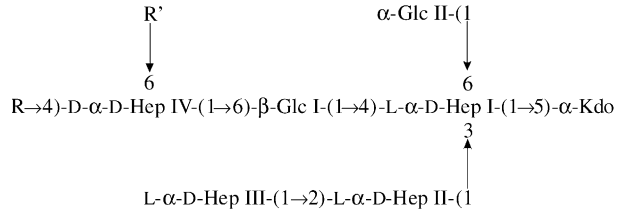


**Figure 8.** Structural representation of the core oligosaccharides from *Ap* serotypes 1, 2, 5a and 5b. For serotype 1; R is (1*S*)-Gal*a*NAc-(1→4,6)-α-Gal II-(1→3)-β-Gal I-(1→, and R′ is H. For serotype 2; R is β-Glc III-(1→, and R′ is D-α-D-Hep V-(1→. For serotypes 5a and 5b; R is H and R′ is D-α-D-Hep V-(1→. All sugars are in the pyranose ring form apart from the open-chain *N*-acetylgalactosamine.

prompted more sophisticated NMR studies to attempt to identify the nature of the presumed HexNAc residue and confirm the linkage pattern for this region of the core OS from serotype 1.

A series of selective 1D experiments from the H-1 $^{1}$H-resonance of the HexNAc residue at 4.88 ppm with mixing times ranging from 30 to 150 ms revealed the H-2 $^{1}$H-resonance at 4.34 ppm and weak signals assigned to H-3 at 4.13 ppm and H-4 at 3.36 ppm. To confirm these inferences and complete assignment of this HexNAc residue further selective experiments were performed. A 1D-TOCSY experiment was obtained from the H-4 $^{1}$H-resonance at 3.36 ppm, which confirmed the H-2 and H-3 assignments and identified the H-5 and H-6,6′ resonances at 3.93, 3.66 and 3.64 ppm, respectively (Fig. 6d). A 1D-NOESY experiment was obtained from the H-2 $^{1}$H-resonance at 4.34 ppm, which confirmed the H-3 and H-4 assignments (Fig. 6e). A 1D-NOESY experiment was obtained from the H-4 $^{1}$H-resonance at 3.36 ppm, which confirmed the H-2, H-3, H-5 and H-6,6′ assignments (Fig. 6f). The coupling constants were determined from these experiments and found to be $J_{1,2}$ 4.8 Hz, $J_{2,3}$ 1.0 Hz, $J_{3,4}$ 9.7 Hz, $J_{4,5}$ 1.4 Hz, $J_{5,6}$ 6.5 Hz, $J_{5,6'}$ 6.5 Hz and $J_{6,6'}$-12 Hz. A 2D-$^{13}$C–$^{1}$H-HSQC NMR spectrum was performed (Fig. 6a) that identified the $^{13}$C chemical shifts for the C-1 to C-6 positions on the HexNAc molecule as 101.1, 52.6, 68.5, 70.0, 70.7 and 64.1 ppm, respectively. This data was initially confusing; however, a search of an in-house carbohydrate database identified a similar set of data for an open-chain *N*-acetylgalactosamine residue found in the core OS from a *Proteus* species.[16,22] The identification of an open-chain residue, although surprising, was consistent with the sugar, methylation and FABMS analysis data, as such a residue would be sensitive to the hydrolysis conditions employed for the sugar and methylation analyses. The formation of a glycosyl oxonium ion for the terminal residue, in FABMS analysis, would be precluded by the open-chain configuration of this residue. This identification also enabled the correct configuration for this residue to be determined as (1*S*) as has been reported previously, and not the original α-configuration inferred from the chemical shift of the H-1 resonance that is not applicable for an open-chain residue.

Structural analysis of the core OS's from the 1, 2, 5a and 5b serotypes was therefore complete and had identified a conserved inner core structure in all strains with different decoration beyond this conserved structure as illustrated in Figure 8.

## 3. Discussion

Structural analysis of core oligosaccharides from serotypes 1, 2, 5a and 5b representing core types I, II, II and II, revealed a relatively conserved structure. The inner core OS was identical for each strain consisting of a trisaccharide of L-*glycero*-D-*manno*-heptose residues linked to a Kdo residue, wherein the proximal heptose residue (Hep I) was substituted at the 3-position by the second L-*glycero*-D-*manno*-heptose residue (Hep II) of the L-*glycero*-D-*manno*-heptose trisaccharide, at the 4-position by a β-glucose residue (Glc I) and at the 6-position by an α-glucose residue (Glc II). A D-*glycero*-D-*manno*-heptose residue (Hep IV) was found at the 6-position of the Glc I residue in each strain, and an L-*glycero*-D-*manno*-heptose residue (Hep III), at the 2-position of Hep II completing the conserved inner core OS structure. A second D-*glycero*-D-*manno*-heptose residue (Hep V) substitutes Hep IV at the 6-position in serotypes 2, 5a and 5b. The only difference between serotypes 2 and 5a, 5b was an additional glucose residue linked to the 4-position of the Hep IV residue in serotype 2. There was a striking similarity between these OS structures and that found previously for the OS from *M. haemolytica* serotype A1.[14] The only difference between the 5b, 5a OS structures and *M. haemolytica* serotype A1 core OS was the absence of the additional terminal galactose residue at Hep V found in *M. haemolytica* A1 OS. In serotype 1 there is no Hep V residue; Hep IV is alternatively substituted at the

4-position by a trisaccharide of (1*S*)-Gal*a*NAc-(1→4,6)-α-Gal-(1→3)-β-Gal-, wherein the GalNAc residue was of the rarely encountered open-chain configuration. The structural arrangement identified as the initial trisaccharide extension from Hep I in serotype 1 is identical to that previously found for *Haemophilus ducreyi* strain 2665 LPS;[23] however, the serotype 1 LPS has a different extension beyond the Gal I residue when compared to the DD-Hep interrupted lacto-*N*-neotetraose structure found in *H. ducreyi*.

A structural explanation has therefore been attained for the SDS-PAGE observation of two core types in *Ap* LPS.[10] Serotypes 2, 5a and 5b of core type II have very similar LPS structures, differing only by an additional glucose residue in serotype 2. However, serotype 1 of core type I has lost a DD-Hep residue, but gained two hexoses and a novel open-chain GalNAc residue. To investigate if this novel open-chain GalNAc residue was found in other core type I serotypes we examined LPS from serotypes 6, 9 and 11. Evidence for the open-chain GalNAc was seen by both MS and NMR studies (data not shown) in serotypes 9 and 11, but not in serotype 6. Closer examination of SDS-PAGE profiles that had been used to categorise core types revealed that serotype 6 had both LPS migration patterns of the two core types, and therefore it is possible that the serotype 6 strain we examined only had a core type II profile.[10]

Little data is available on the genetic control of LPS biosynthesis in *Ap*. A recent paper by Galarneau et al.[24] identified three genes following transposon mutagenesis that appeared to be involved in the biosynthesis of the core OS region of *Ap* serotype 1 LPS. These genes were tentatively identified as glycosyltransferases based on homology to other glycosyltransferases. The three genes were postulated to be *lbgB*, an α-(1→6)-DD-heptosyltransferase, *lbgA* a β-(1→4)-galactosyltransferase and a hexose or *N*-acetylhexosamine transferase. The former two genes, *lbgAB*, are consistent with the structure identified here in serotype 1 core OS, and have the same locus arrangement as found in *H. ducreyi* LPS.[25] Another paper by Rioux et al.[9] identified a gene *galU*, the structural gene for UTP-α-D-glucose-1-phosphate uridyltransferase. SDS-PAGE of LPS isolated from a serotype 1 *Ap galU* mutant strain had an altered migration pattern of the core-lipid A region, and this mutant strain, which was less adherent to pig tracheal cells, was less virulent in pigs, suggesting that an alteration in the nature or presentation of the core OS region could have an effect on the virulence of this animal pathogen.

The identification of an open-chain GalNAc residue was of interest. This structure has only previously been identified in two Proteus species[16,22] and recently in *Shewanella oneidensis*,[26] and its significance is unknown. As found in the existing literature, the open-chain residue identified here was found to concurrently di-substitute the neighbouring residue at the 4- and 6-positions, so this could be a common arrangement for such residues. The apparent absence of the GalNAc residue in the sugar and methylation analyses is also consistent with previous data for such an open-chain residue, whereby if the residue is terminal it is not observed.[26]

The identification of a DD-Hep residue in the oligosaccharide extension from Hep I has been observed before for several strains including *M. haemolytica*, *H. ducreyi* and nontypable *H. influenzae*.[14,23,27] In *M. haemolytica* two DD-Hep residues were observed, whereas in *H. ducreyi* and *H. influenzae* only one DD-Hep residue was found. In *Ap* both scenarios exist, with serotypes 2 and 5a, 5b having two DD-Hep residues and serotype 1 having just one DD-Hep residue in the oligosaccharide extension from Hep I. The tri-LD-heptosyl inner core group has also been observed previously in *M. haemolytica*, *H. ducreyi* and *H. influenzae*.[14,23,28] The 3,4,6-trisubstituted Hep I residue found here for all strains of *Ap* studied has been observed before in *M. haemolytica* LPS; however, *H. ducreyi* LPS only elaborates the 3,4-di-substituted Hep I residue as also found in *H. influenzae*.

The identification of the 7-position of the Hep III residue as the point of attachment of the O-antigen galactose residue in serotype 5a was of interest. This is consistent with the observation that three variously truncated core oligosaccharide mutants in serotype 1 still elaborated an O-antigen,[24] as the anticipated function of the three mutated gene products would not interfere with the biosynthesis of the inner core LD-heptosyl trisaccharide unit and therefore the acceptor for O-antigen attachment would still be present in the mutant LPS core oligosaccharide.

This study has structurally characterised the core oligosaccharide region of several strains of *Ap*, which are representative of the two core types, and serve to identify a conserved inner-core structure and a novel outer-core constituent. This region is known to be involved in the adherence of *Ap* and is therefore implicated in virulence. This study will therefore better enable future studies on the relevance of the structure of the core oligosaccharide region of *Ap* LPS to the potential virulence of this organism.

## 4. Materials and methods

### 4.1. Media and growth conditions

*Ap* serotypes 1 (strain 4074), 2 (strain 4226), 5a (strain K17) and 5b (strain L20) were initially grown for 16 h on chocolate agar plates at 37 °C and growths were used to inoculate 1 L of brain–heart infusion (BHI) medium supplemented with β NAD (Sigma N-7004) to a final

concentration of 5 μg/mL, haemin (Sigma H-2250) to a final concentration of 5 μg/mL and 1% glucose (10 g). Cultures were then incubated at 37 °C at 200 rpm for 6 h and used to inoculate 23 L of BHI medium (supplemented as above) in a 28-L NBS fermenter. The cultures were then grown at 37 °C, with 24 L/min aeration and stirring at 200 rpm for 18 h. Cells were killed (2% phenol w/v, for 4 h) and harvested by using a Sharples continuous centrifuge (~40 g wet weight).

### 4.2. Isolation, purification and degradation of the lipopolysaccharide

The lipopolysaccharide (LPS) was isolated from the dried cell mass by the hot water–phenol method,[29] following washing of the dried cell mass with organic solvents for serotypes 5a and 5b.[15] The aqueous phase was dialysed against water and lyophilised and in the case of serotype 2, the LPS was isolated from the extensively dialysed phenol phase.[19] The dried sample was dissolved in water to give a 1–2% solution (w/v) and treated with deoxyribonuclease I (DNase) (0.01 mg/mL) and ribonuclease (RNase) (0.01 mg/mL) for 3 h at 37 °C, then treated with proteinase K (0.01 mg/mL) for 3 h. The dialysed, dried sample was dissolved in water to make a 1% solution and ultracentrifuged (5 h, 100,000 × *g*). The LPS pellet was redissolved in water and lyophilised, purified by gel-filtration on a column of Bio-Gel P-2 (1 cm × 100 cm) with water as eluent, and fractions containing sugar were pooled and lyophilised. Purified LPS was treated with anhydrous hydrazine with stirring at 37 °C for 1 h to prepare O-deacylated LPS (LPS-OH). The reaction mixture was cooled in an ice bath, and gradually, cold acetone (−70 °C, 5 vols.) was added to destroy excess hydrazine and the precipitated LPS-OH was isolated by centrifugation. The sample was then purified down a Bio-Gel P-2 column as described above. The core oligosaccharide (OS) was isolated by treating the purified LPS with 1% HOAc (10 mg/mL, 100 °C, 1.5 h) with subsequent removal of the insoluble lipid A by centrifugation (5000 × *g*). The lyophilised OS was further purified down a Bio-Gel P-2 column with individual fractions lyophilised.

### 4.3. Analytical methods

Sugars were determined as their alditol acetate derivatives[30] by GLC–MS. Samples were hydrolysed for 4 h using 4 M trifluoroacetic acid at 100 °C. The hydrolysate was reduced ($NaBD_4$) for 16 h in $H_2O$ and acetylated with $Ac_2O$ at 100 °C for 2 h using residual NaOAc as catalyst. The GLC–MS was equipped with a 30 m DB-17 capillary column (180–260 °C at 3.5 °C/min), and MS was performed in the electron-impact mode on a Varian Saturn II mass spectrometer. Methylation analysis was carried out by the NaOH–DMSO–MeI procedure[31] and analysed by GLC–MS as above. Absolute configurations were determined by GLC analysis of *sec*-butylglycoside derivatives.[32]

### 4.4. Mass spectrometry

ESIMS was performed in the negative-ion mode on a VG Quattro Mass Spectrometer (Micromass, Manchester, UK) by direct infusion of samples in 25% aq acetonitrile containing 0.5% HOAc. Capillary electrophoresis CE-ESIMS was performed on a crystal Model 310 (CE) instrument (AYI Unicam) coupled to an API 3000 mass spectrometer (Perkin–Elmer/Sciex) via a microIonspray interface. A sheath solution (2:1 2-PrOH–MeOH) was delivered at a flow rate of 1 μL/min to a low dead volume tee (250 μm i.d., Chromatographic Specialties). All aq sols were filtered through a 0.45-μm filter (Millipore) before use. An electrospray stainless steel needle (27 gauge) was butted against the low dead volume tee and enabled the delivery of the sheath solution to the end of the capillary column. The separations were obtained on about a 90-cm length of bare fused-silica capillary using 10 mM ammonium acetate–ammonium hydroxide in deionised water, pH 9.0, containing 5% MeOH. A voltage of 20 kV was typically applied at the injection. The outlet of the capillary was tapered to ca. 15 μm i.d. using a laser puller (Sutter Instruments). Mass spectra were acquired with dwell times of 3.0 ms per step of 1 $m/z$ unit in full-mass scan mode. The MS/MS data were acquired with dwell times of 1.0 ms per step of 1 $m/z$ unit. Fragment ions formed by collision activation of selected precursor ions with nitrogen in the RF-only quadrupole collision cell, were mass analysed by scanning the third quadrupole.

### 4.5. Nuclear magnetic resonance spectroscopy

NMR experiments were acquired on Varian Inova 400, 500 and 600 MHz spectrometers using a 5- or 3-mm triple resonance ($^1H$, $^{13}C$, $^{31}P$) probe. The lyophilised sugar sample was dissolved in 600 μL (5 mm) or 140 μL (3 mm) of 99% $D_2O$. The experiments were performed at 25 °C with suppression of the HOD (deuterated $H_2O$) signal at 4.78 ppm. The methyl resonance of acetone was used as an internal reference at 2.225 ppm for $^1H$ spectra and 31.07 ppm for $^{13}C$ spectra. Standard homo and heteronuclear correlated 2D pulse sequences from Varian, COSY, TOCSY, NOESY, $^{13}C$–$^1H$ HSQC, $^{13}C$–$^1H$ HSQC–TOCSY and $^{13}C$–$^1H$ HMBC, were used for general assignments. Selective 1D-TOCSY with a Z-filter and 1D-NOESY experiments and 1D analogues of 3D-NOESY–TOCSY and TOCSY–NOESY experiments were performed for complete residue assignment and for the determination of $^1H$–$^1H$ nuclear Overhauser

enhancements.[33] The pulse width of the selective pulses was 30–80 Hz. Mixing times of 30–150 ms were used for the 1D-TOCSY experiments. Mixing times of 400–800 ms were used for the 1D-NOESY experiments.

## Acknowledgements

The authors would like to thank Perry Fleming and Doug Griffith for cell growth, and Kenneth Chan and Lisa Morisson for mass spectrometry.

## References

1. Taylor, D. J. In *Diseases of Swine*, 8th ed.; Straw, B. E., D'Allaire, S., Mengeling, W. L., Taylor, D. J., Eds.; Iowa State University Press: Ames, 1999; pp 343–354.
2. Frey, J. *Trends Microbiol.* **1995**, *3*, 257–261.
3. Haesebrouck, F.; Chiers, K.; Van Overbeke, I.; Ducatelle, R. *Vet. Microbiol.* **1997**, *58*, 238–249.
4. Bossé, J. T.; Janson, H.; Sheehan, B. J.; Beddek, A. J.; Rycroft, A. N.; Kroll, J. S.; Langford, P. R. *Microbes Infect.* **2002**, *4*, 225–235.
5. Blackall, P. J.; Klaasen, H. L. B. M.; van den Bosch, H.; Kuhnert, P.; Frey, J. *Vet. Microbiol.* **2002**, *84*, 47–52.
6. Perry, M. B.; Altman, E.; Brisson, J.-R.; Beynon, L. M.; Richards, J. C. *Serol. Immunother. Infect. Dis.* **1990**, *4*, 299–308.
7. Belanger, M.; Dubreuil, D.; Harel, J.; Girard, C.; Jacques, M. *Infect. Immun.* **1990**, *58*, 3523–3530.
8. Paradis, S.; Dubreuil, D.; Rioux, S.; Gottschalk, M.; Jacques, M. *Infect. Immun.* **1994**, *62*, 3311–3319.
9. Rioux, S.; Galarneau, C.; Harel, J.; Frey, J.; Nicolet, J.; Kobisch, M.; Dubreuil, J. D.; Jacques, M. *Can. J. Microbiol.* **1999**, *45*, 1017–1026.
10. Jacques, M.; Rioux, S.; Paradis, S.-E.; Begin, C.; Gottschalk, M. *Can. J. Microbiol.* **1996**, *42*, 855–858.
11. Altman, E.; Brisson, J.-R.; Gagne, S. M.; Perry, M. B. *Eur. J. Biochem.* **1992**, *204*, 225–230.
12. Cox, A. D.; Li, J.; Richards, J. C. *Eur. J. Biochem.* **2002**, *269*, 4169–4175.
13. Li, J.; Bauer, S. H. J.; Mansson, M.; Moxon, E. R.; Richards, J. C.; Schweda, E. K. H. *Glycobiology* **2001**, *11*, 1009–1015.
14. Brisson, J.-R.; Crawford, E.; Uhrin, D.; Khieu, N. H.; Perry, M. B.; Severn, W. B.; Richards, J. C. *Can. J. Chem.* **2002**, *80*, 949–963.
15. Masoud, H.; Moxon, E. R.; Martin, A.; Krajcarski, D.; Richards, J. C. *Biochemistry* **1997**, *36*, 2091–2103.
16. Vinogradov, E.; Bock, K. *Carbohydr. Res.* **1999**, *320*, 239–243.
17. Romanowska, E.; Gamian, A.; Lugowski, C.; Romanowska, A.; Dabrowski, J.; Hauck, M.; Opferkuch, H. J.; von der Lieth, C.-W. *Biochemistry* **1988**, *27*, 4153–4161.
18. Backman, I.; Erbing, B.; Jansson, P.-E.; Kenne, L. *J. Chem. Soc., Perkin Trans. 1* **1988**, 889–898.
19. Altman, E.; Brisson, J.-R.; Bundle, D. R.; Perry, M. B. *Biochem. Cell Biol.* **1987**, *65*, 876–889.
20. Altman, E.; Brisson, J.-R.; Perry, M. B. *Biochem. Cell Biol.* **1987**, *65*, 414–422.
21. Altman, E.; Brisson, J.-R.; Perry, M. B. *Biochem. Cell Biol.* **1986**, *64*, 1317–1325.
22. Vinogradov, E.; Bock, K. *Angew. Chem., Int. Ed.* **1999**, *38*, 671–674.
23. Schweda, E. K. H.; Sundstrom, A. C.; Eriksson, L. M.; Jonasson, J. A.; Lindberg, A. *J. Biol. Chem.* **1994**, *269*, 12040–12048.
24. Galarneau, C.; Rioux, S.; Jacques, M. *Pathogenesis* **2000**, *1*, 253–264.
25. Tullius, M. V.; Phillips, N. J.; Scheffler, N. K.; Samuels, N. M.; Munson, R. S., Jr.; Hansen, E. J.; Stevens-Riley, M.; Campagnari, A. A.; Gibson, B. W. *Infect. Immun.* **2002**, *70*, 2853–2861.
26. Vinogradov, E.; Korenevsky, A.; Beveridge, T. J. *Carbohydr. Res.* **2003**, *338*, 1991–1997.
27. Rahman, M. M.; Gu, X.-X.; Tsai, C.-M.; Kolli, V. S. K.; Carlson, R. W. *Glycobiology* **1999**, *9*, 1371–1380.
28. Cox, A. D.; Masoud, H.; Thibault, P.; Brisson, J.-R.; van der Zwan, M.; Perry, M. B.; Richards, J. C. *Eur. J. Biochem.* **2001**, *268*, 5278–5286.
29. Westphal, O.; Jann, K. *Methods Carbohydr. Chem.* **1965**, *5*, 88–91.
30. Sawardeker, D. G.; Sloneker, J. H.; Jeanes, A. *Anal. Chem.* **1965**, *37*, 1602–1604.
31. Ciucanu, I.; Kerek, F. *Carbohydr. Res.* **1994**, *131*, 209–217.
32. Vinogradov, E. V.; Holst, O.; Thomas-Oates, J. E.; Broady, K. W.; Brade, H. *Eur. J. Biochem.* **1992**, *210*, 491–498.
33. Brisson, J. R.; Sue, S. C.; Wu, W. G.; McManus, G.; Nghia, P. T.; Uhrin, D. In *NMR Spectroscopy of Glycoconjugates*; Jimenez-Barbero, J., Peters, T., Eds.; Wiley-VCH: Weinhem, 2002; pp 59–93.